Institute of Paper Science and Technology
Atlanta, Georgia

IPST TECHNICAL PAPER SERIES

NUMBER 380

SOUND WAVE DISPERSION AND ATTENUATION IN THE THICKNESS DIRECTION OF PAPER

P.H. BRODEUR AND M.S. HALL

JUNE, 1991

Sound Wave Dispersion and Attenuation in the Thickness Direction of Paper

P.H. Brodeur and M.S. Hall

To be presented at
1991 International Paper Physics Conference
September 22–27, 1991
Kona, Hawaii

SOUND WAVE DISPERSION AND ATTENUATION IN THE THICKNESS DIRECTION OF PAPER

P.H. Brodeur and M.S. Hall
Institute of Paper Science and Technology
Atlanta, Georgia 30318 U.S.A.

ABSTRACT

Sound waves propagating in solid materials are subjected to two phenomena: dispersion and attenuation. While dispersion refers to sound velocity dependency upon frequency, attenuation is described as the wave amplitude decreasing with distance. Since these phenomena are closely related, dispersion measurements can be used to predict attenuation data as a function of frequency, and vice versa. In this paper, sound dispersion and attenuation in the thickness direction of paper are investigated at ultrasonic frequencies. Using a non-destructive ultrasonic transmission technique based on transducers immersed in water-filled rubber wheels, thickness direction ultrasonic wave propagation measurements are performed. From the time delay analysis of the transmitted ultrasonic signals gathered with and without a paper specimen in the nip between the wheels, caliper, travelling time through paper, ZD longitudinal sound velocity, and ZD elastic modulus are determined. Frequency domain analysis provides the necessary information for evaluation of sound dispersion and attenuation effects. Results are presented for a 69 lb linerboard specimen. It is found that dispersion at frequencies less than 1.25 MHz is weak and approximately linear for this specimen. The frequency dependent ZD elastic modulus is predicted in the vicinity of the zero frequency. The directly measured and dispersion predicted attenuation coefficients as a function of frequency are in good agreement up to 1.25 MHz. The sound reflection coefficient as determined from the comparative analysis of the attenuation coefficients is abnormally high. This suggests that poor coupling between the specimen and the rubber wheels accounts for most of the observed loss in signal strength.

KEYWORDS: Ultrasonic wave propagation in paper, sound velocity, dispersion, attenuation, reflection, caliper, elastic modulus.

INTRODUCTION

Sound wave dispersion and attenuation in solid materials and sound wave reflection at the surface of solid materials are physical phenomena typically studied on specimens immersed in a water tank. In these studies, immersion acoustic coupling is necessary to transfer ultrasonic waves from a source (transmitting transducer) into the tested material and then from this material to a detector (receiving transducer). Obviously, non-destructive immersion characterization with paper specimens is not possible. Dry, hard-platen contact coupling is also ineffective because unavoidable air-filled gaps between the transducers and the material under investigation are impenetrable to ultrasonic waves. Fortunately, rubber materials conform with paper surface irregularities and thus offer a good compromise between immersion coupling and dry, hard-platen coupling. Caliper and thickness direction sound velocity were successfully measured with a soft-platen neoprene interface between ultrasonic probes and paper specimens.[1,2,3]

Recently, on-line, non-destructive ultrasonic-based techniques aimed at inferring thickness direction strength properties of paper materials from elastic stiffness measurements were investigated.[4] One of these techniques, based on sensors immersed in water-filled rubber wheels, has emerged as a strong candidate for continuous monitoring implementation. The water-filled rubber wheels technique allows non-destructive determination of caliper and travelling time in paper, from which thickness direction longitudinal sound velocity is evaluated. Additional information on sound dispersion, attenuation and reflection can be gathered from the frequency domain amplitude and phase spectra of the detected ultrasonic signals. Generally speaking, sound dispersion and attenuation in solid materials are related phenomena. It is known that dispersion and attenuation can be connected by the Kramers-Kronig relations.[5,6] These relations can be used to predict attenuation from dispersion, and vice versa.

Sound dispersion in paper was studied previously with broadband PVDF transducers and it was shown that dispersion is weak at frequencies less than 2 MHz.[2] The decrease in sound attenuation was used to evaluate the effect of sizing agents in paper specimens upon contact with water.[7,8] Neoprene-faced PVDF transducers were developed to couple ultrasound into solids and to evaluate the reflection coefficient from direct pulse-echo measurements.[3] Results were not satisfactory. To the knowledge of the authors, a self-contained study of sound dispersion, attenuation and reflection phenomena in paper materials as a function of frequency is not yet available.

It is the purpose of this paper to present the findings of a preliminary investigation of dispersion and attenuation using an approach based on frequency domain analysis of ultrasonic signals propagating through paper specimens. This paper is structured as follows: Measurement principles using the water-filled rubber wheels technique are first introduced. Next, principles of dispersion, attenuation and reflection are presented. The experimental procedure is briefly described. Demonstration measurements for a 69 lb linerboard specimen are then reported and followed by a summary.

MEASUREMENT PRINCIPLES USING THE WATER-FILLED WHEELS TECHNIQUE

Figure 1 shows a photograph of the water-filled wheels setup used to study dispersion, attenuation and reflection phenomena. A paper specimen is inserted in the nip between the wheels. In the present case, wheels are made with molded urethane (hard-rubber). A schematic of the measurement technique is presented in Figure 2. Two ultrasonic transducers mounted in the hub of the wheels, a transmitter and a receiver, are used in a transmission mode configuration. Water is used to acoustically couple the stationary transducers and the free-to-rotate wheels. In some ways, the water-filled wheels setup has some similarities with a typical water tank setup, with the exception of the necessary dry coupling with paper. Since the transducer separation distance is constant, the sound path in water is decreased by an amount equivalent to the thickness of the paper specimen. As the signal launched from the transmitter travels through water, rubber, paper, and then rubber and water, one directly transmitted signal and several interface reflection time-delayed signals are collected by the receiver. Only a few of the time-delayed signals can provide useful information.

Caliper and ZD Longitudinal Sound Velocity

Signals #1 and #2 depicted in Figure 2 are of particular interest. They can be used to simultaneously evaluate the caliper, Δd, and the sound travelling time, Δt, through paper. Mathematical details for the measurement technique are reported elsewhere.[9] They are summarized here. Assuming that the composite sound velocity, v_f, in the wheels (water and rubber paths) is a known quantity, it can be shown that Δd is

$$\Delta d = v_f [\delta t_{21} - \delta t_{2'1'}] / 2 \qquad (1)$$

where $\delta t_{21} = t_2 - t_1$ and $\delta t_{2'1'} = t_{2'} - t_{1'}$ are the time differences between signals #1 and #2 collected without and with a specimen in the nip, respectively. The travelling time through paper is

$$\Delta t = \delta t_{1'1} + \Delta d / v_f \qquad (2)$$

in which $\delta t_{1'1} = t_{1'} - t_1$ is the time difference for signal #1 recorded with and without a specimen in the nip. From the ratio of (1) and (2), the thickness direction longitudinal sound velocity is

$$v_z = \Delta d / \Delta t \quad (3)$$

v_z is related to the elastic modulus, E_z, and the sheet density, ρ, such that

$$v_z^2 = E_z / \rho \quad (4)$$

PRINCIPLES OF SOUND DISPERSION, ATTENUATION AND REFLECTION

Dispersion, Phase Velocity and Group Velocity

In the above treatment, it was assumed that v_z is frequency independent. A more fundamental analysis of v_z would indicate that this is not so. Unlike metals, which have homogeneous structures, paper materials are highly heterogeneous media. Thus, they should exhibit dispersion, i.e., a change of sound velocity with frequency. Sound velocity as a function of frequency is usually defined as the phase velocity $v_p(f)$. Using an adaptation of the dispersion analysis by Lee et al.[5] for solid specimens immersed in a water tank, the phase velocity for the water-filled wheels setup may be described as:

$$v_p(f) = \omega/\beta = v_f/\{1 + (v_f\Delta\phi(f)) / (2\pi f \Delta d)\} \quad (5)$$

where $\Delta\phi(f) = \phi_r(f) - \phi_s(f)$ is the phase difference between the "reference" phase $\phi_r(f)$, which is the phase frequency spectrum for signal #1 (see Figure 2) recorded without a specimen in the nip, and the "specimen" phase $\phi_s(f)$. $\omega = 2\pi f$ is the angular frequency and β is the specimen propagation constant. At zero frequency, the phase difference is zero (no wave propagation) and the phase velocity is indeterminate. Dispersion is negligible in water and rubber (urethane in the present case) at low MHz frequencies. Hence, any measurable dispersion effect in this frequency range should be due to paper. Sound velocity as defined by equation (4) is valid if dispersion is weak. We can also define the group velocity which corresponds to the rate of change of the phase velocity as signal #1 propagates through the specimen. The group velocity is:

$$v_g(f) = d\omega/d\beta = v_f/\{1 + (v_f/(2\pi \Delta d))(d[\Delta\phi(f)] / df)\} \quad (6)$$

For a non-dispersive material $v_g(f)$ is equal to $v_p(f)$.

Attenuation and Reflection

A decrease of wave amplitude with distance as ultrasonic waves propagate through a material is described as sound attenuation. Two mechanisms are responsible for attenuation: absorption, which is related to the material structure, and scattering, which is related to the material component dimensions with respect to the ultrasonic wavelength. Although not demonstrated yet, the scattering mechanism is most likely responsible for complete sound extinction at frequencies near 2 to 3 MHz in paper because ultrasonic wavelengths are comparable to fiber dimensions at these frequencies. In a transmission arrangement like the water-filled wheels setup, the measured sound attenuation must be related to the fraction of the incident signal reflected at the surface of the tested specimen. Assuming an identical reflection coefficient R on both sides of the paper sample, the sound attenuation coefficient as a function of frequency is given by

$$\alpha(f) = (-1 / \Delta d) \ln\{(U_s(f) / U_r(f)) / (1 - R^2)\} \quad (7)$$

where $U_r(f)$ and $U_s(f)$ are the reference and specimen amplitude frequency spectrum, respectively. For an unbounded material, sound attenuation is the sufficient and necessary condition to develop dispersion. It is known that sound dispersion and attenuation can be related mathematically. Attenuation can be predicted from dispersion, and vice versa. The so-called Kramers-Kronig relations relating dispersion and attenuation have been validated experimentally for highly attenuative specimens immersed in water.[5] Assuming that these relations also hold for paper materials, the dispersion predicted attenuation coefficient is

$$\alpha(f) = (-\pi f^2 / (2\Delta d))\, d[\Delta\phi(f) / f] / df \quad (8)$$

Equations (7) and (8) can be equated to predict the reflection coefficient from dispersion and attenuation measurements.

EXPERIMENTAL PROCEDURE

Referring to Figure 2, two identical, unfocused immersion-type, narrowband piezoelectric ceramic transducers were used to launch and receive ultrasonic signals. One full-cycle sinewave at 1 MHz, produced by a wave function generator, was used as the incident signal. It was amplified with a wide-band power amplifier. Since the transducer's bandwidth is centered near 1 MHz, the frequency content of the incident pulse was ultimately determined by the transmitter bandwidth. The received waveforms of interest (see Figure 2) were preamplified and captured on a one-to-one basis with a GPIB controlled 2432 Tektronix scope. Time resolution, record length and vertical resolution were 10 ns, 1kB, and 8 bits, respectively. Signal averaging (32 successive acquisitions) was used to improve the signal-to-noise ratio. Collected waveforms were transferred to a 386 computer for later analysis. A cross-correlation technique was used to determine the caliper and the ZD longitudinal sound velocity.[9] Investigation of the frequency content of the directly transmitted signal, captured without and with a specimen in the nip between the wheels, was accomplished with a fast Fourier transform procedure. All measurements were made at 50% RH and 23 ^{o}C.

RESULTS

Caliper and ZD Longitudinal Sound Velocity

For demonstration purposes, measurements are reported for a 69 lb linerboard specimen. This specimen was selected on the basis that it exhibits measurable dispersion and attenuation around 1MHz (fine papers show very little dispersion at this frequency). The caliper and ZD longitudinal sound velocity as determined with equations (1) and (3) were 458 μm and 232 m/s, respectively. Those figures are in good agreement with the results obtained with the IPST ZD soft-platen ultrasonic laboratory instrument (466 μm and 239 m/s, respectively).

Frequency Domain Analysis

Consider the time domain waveforms illustrated in Figure 3. As previously defined, the reference waveform corresponds to the directly transmitted signal (#1 in Figure 2) recorded without a specimen in the nip. It is seen that the specimen waveform is delayed with respect to the reference waveform because sound velocity in paper is much less than that in water (1486 m/s at room temperature). The specimen waveform amplitude is strongly attenuated.

Using the fast Fourier transform procedure, the amplitude and phase spectra were determined as a function of frequency for both reference and specimen waveforms. The amplitude (U) and phase (ϕ) are displayed in Figures 4 and 5, respectively. Looking first at the amplitude curves, we observe a large change in amplitude due to sound attenuation in the specimen. This is in agreement with the amplitude change denoted in the time domain (Figure 3). The maximum amplitude frequency for the reference signal is 0.81 MHz. This is slightly less than the measured maximum amplitude frequency response for the transducers (actually 0.95 MHz). The shift toward a lower frequency for the specimen maximum amplitude frequency (0.63 MHz) is an indication of the sound attenuation dependency upon frequency. Analyzing now the phase results (Figure 5), the relative linearity of the specimen phase with respect to the reference phase indicates that dispersion is approximately linear in the tested specimen. The slope of the reference phase is arbitrary. The larger negative slope for the specimen phase is in agreement with the longer travelling time in paper.

Dispersion

Using the reference and specimen phase spectra shown in Figure 5, the phase difference $\Delta\phi(f)$ is easily calculated. It is presented in Figure 6 (dotted line). Neglecting end effects below 0.25 MHz and above 1.25 MHz due to poor signal-to-noise ratio in these regions, we observe that the phase difference is approximately linearly related to the frequency in the tested frequency range. In order to get an analytical expression for the phase difference, a second order polynomial curve fitting was performed between 0.25 and 1.25 MHz. From physical considerations, the phase difference must be zero at zero frequency. Hence, the fitted curve intercept was reset to zero. The corrected fitted phase difference is represented by the solid line in Figure 6.

Using equations (5) and (6), the phase and group velocities were computed. Results are plotted as a function of frequency in Figure 7. The phase velocity increases approximately linearly by 7.5% from 0.25 to 1.25 MHz. Therefore, the dispersion is weak but measurable. As a means of comparison, the ZD longitudinal sound velocity, 232 m/s, is included in the graph (short-dashed line). This frequency-independent result is an approximation to the phase velocity. It is interesting to see that the phase velocity can be extrapolated below 0.25 MHz (excluding the zero frequency) and above 1.25 MHz. Measurements at frequencies above 1.25 MHz are necessary to verify or dismiss the predicted dispersion trend. As expected from dispersion consideration, the group velocity is different from the phase velocity. In the vicinity of the zero frequency, dispersion is negligible and $v_g(f) \to v_p(f)$.

Replacing v_z by $v_p(f)$ in equation (4), we can evaluate the elastic modulus as a function of frequency, i.e., $E_z(f)$. Assuming a measured density of 712 kg/m^3 for the tested paper sample, the elastic modulus spectrum is presented in Figure 8. The dashed line represents the frequency independent elastic modulus (38.3 MPa). The predicted elastic modulus in the vicinity of the zero frequency is at a minimum (31.7 MPa). It is known from previous studies that the in-plane elastic moduli measured acoustically are larger than the elastic moduli obtained from destructive tensile testing at zero frequency.[10,11] The present analysis supports this trend, but in the thickness direction. ZD tensile measurements were not performed on the linerboard specimen.

Attenuation and Reflection

The measured attenuation coefficient as a function of frequency was calculated using equation (7) and the amplitude spectra shown in Figure 4. Equation (8) and the phase difference spectrum (Figure 6) were used to calculate the dispersion predicted attenuation coefficient. Results in decibel per micrometer are plotted in Figure 9. The solid line refers to the predicted attenuation. The long-dashed line represents the measured attenuation when the reflection coefficient R is set to zero in equation (7), and the short-dashed line corresponds to the measured attenuation when R is used as a fitting parameter. Neglecting end effects once again, the correlation is generally good between the measured and predicted attenuation coefficients in the frequency range of interest.

The reflection coefficient used in the fitting process is shown in Figure 10. It is interesting to note that R does not significantly vary with frequency. Its average value is 0.885, indicating that 88.5% of the incident wave is reflected. This value seems to be abnormally high. In order to verify its validity, a pulse-echo experiment was devised to determine R directly from the reflected signal at one of the rubber-paper interfaces. The acoustic impedances of hard-rubber and paper are so different that reflection measurements failed to detect any reflection dependency on paper. Thus, interpretation of the reflection coefficient is problematic. It is most likely that the discrepancy between the measured and predicted attenuation coefficient is essentially due to poor coupling between the wheels and the paper specimen. A short experiment with a metal shim (no attenuation expected in metal at low MHz frequencies) inserted in the nip between the wheels confirms that the transmitted signal is highly attenuated. Attenuation is dramatically reduced when water films are used to improve coupling between the shim and the wheels. Evaluation of the reflection coefficient for paper materials is not an easy task, and hard-rubber coupling is inefficient.

SUMMARY AND CONCLUSIONS

Sound dispersion and attenuation in the thickness direction of a 69 lb linerboard specimen were investigated using ultrasonic sensors immersed in water-filled molded urethane wheels. Fourier transform analysis of the directly transmitted ultrasonic signal gathered without and with the specimen in the nip between the wheels was used to get the amplitude and phase spectra as a function of frequency. It is found that the phase velocity increases by 7.5% from 0.25 to 1.25 MHz. The relationship with frequency is approximately linear. The frequency-independent ZD longitudinal velocity is an approximation to the phase velocity. Since the tested paper specimen is dispersive, the phase and group velocities are different. The phase velocity was used to evaluate the elastic modulus as a function of frequency. Results predict that the elastic modulus is at a minimum in the vicinity of the zero frequency.

The sound attenuation coefficient as a function of frequency was determined directly using wave amplitude information, and indirectly using the Kramers-Kronig relationship connecting dispersion and attenuation. The reflection coefficient was used as a free parameter in the comparative analysis of the measured and predicted coefficients. The predicted attenuation verifies the measured attenuation up to 1.25 MHz. The reflection coefficient is nearly constant from 0.25 to 1.25 MHz. Since its value is close to one, and therefore abnormally high, it is believed that this is an indication of poor coupling between the hard-rubber wheels and the specimen. This hypothesis is supported by the fact that it was not possible to evaluate directly the reflection coefficient using a pulse-echo technique.

Additional measurements with a large array of paper specimens and at frequencies above 1.25 MHz are required to understand the mechanisms for sound dispersion and attenuation in paper, to validate the Kramers-Kronig relationship for paper, and to establish relations with paper physical properties. It would be of particular interest to examine the relationship between attenuation and porosity. Prediction of the elastic modulus near the zero frequency is also an important point that requires future consideration. Acoustic coupling could be improved by using soft-rubber wheels instead of hard-rubber wheels. This could lead to a successful determination of the reflection coefficient.

ACKNOWLEDGEMENTS

This research was supported by member companies of the Institute of Paper Science and Technology and by the U.S. Department of Energy under contract No. DE-AC05-86CE40777. The authors wish to thank T.G. Jackson and K.W. Lorenz for their technical assistance.

LITERATURE CITED

1. W.A. Wink and G. A. Baum, Tappi J., "A Rubber Platen Caliper Gauge - A New Concept in Measuring Paper Thickness," 66 (9): 131-133 (1983).

2. C.C. Habeger and W.A. Wink, J. Appl. Pol. Sc., "Ultrasonic Velocity Measurements in the Thickness Direction of Paper," 32: 4503-4540 (1986).

3. C.C. Habeger, W.A. Wink, and M.L. Van Zummeren, J. Acoust. Soc. Am., "Using Neoprene-Faced, PVDF Transducers to Couple Ultrasound into Solids," 84 (4): 1388-1396 (1988).

4. M.S. Hall, Sensors, "On-Line Ultrasonic Measurement of Paper Strength," 7 (7): 13-20 (1990).

5. C.C. Lee, M. Lahham, and B.G. Martin, IEEE Trans. Ultra. Ferro. Freq. Contr., "Experimental Verification of the Kramers-Kronig Relationship for Acoustic Waves," 37 (4): 286-294 (1990).

6. M. O'Donnel, E.T. Jaynes, and J.G. Miller, J. Acoust. Soc. Am., "Kramers-Kronig Relationship between Ultrasonic Attenuation and Phase Velocity," 69 (3): 696-701 (1981).

7. Y-L. Pan, S. Kuga, M. Usuda, and T. Kadoya, Tappi J., "Ultrasound Can Evaluate Paper Sizing," 68 (9): 98-102 (1985).

8. Y-L. Pan, S. Kuga, and M. Usuda, Tappi J., "An Ultrasonic Technique to Study Wetting and Liquid Penetration of Paper," 71(5): 119-123 (1988).

9. P.H. Brodeur and M.S. Hall, "Thickness Direction Measurements in Paper Materials using Ultrasonic Sensors Embedded in Fluid-Filled Wheels," Proc. 1991 Ultrasonics Inter. Conf., Le Touquet, France (to be published).

10. R.W. Mann, G.A. Baum, and C.C. Habeger, Tappi J., "Determination of All Nine Orthotropic Elastic Constants for Machine-Made Paper," 63(2): 163-166 (1980).

11. B. Castagnede, R.E. Mark, and Y.B. Seo, J. Pulp Paper Sci., "New Concepts and Experimental Implications in the Description of the 3-D Elasticity of Paper. Part 2: Experimental Results," 15(6): J201-J205 (1989).

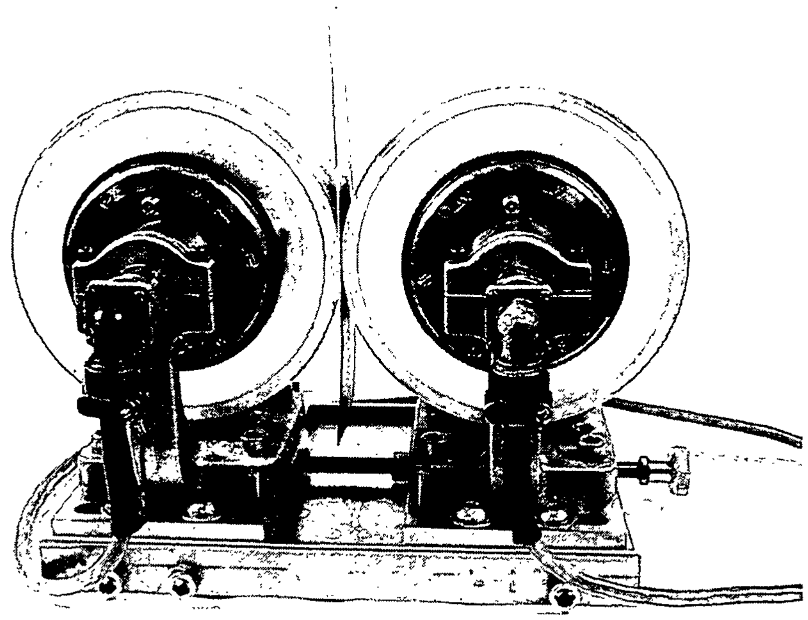

Figure 1: Photograph of the water-filled rubber wheels setup.

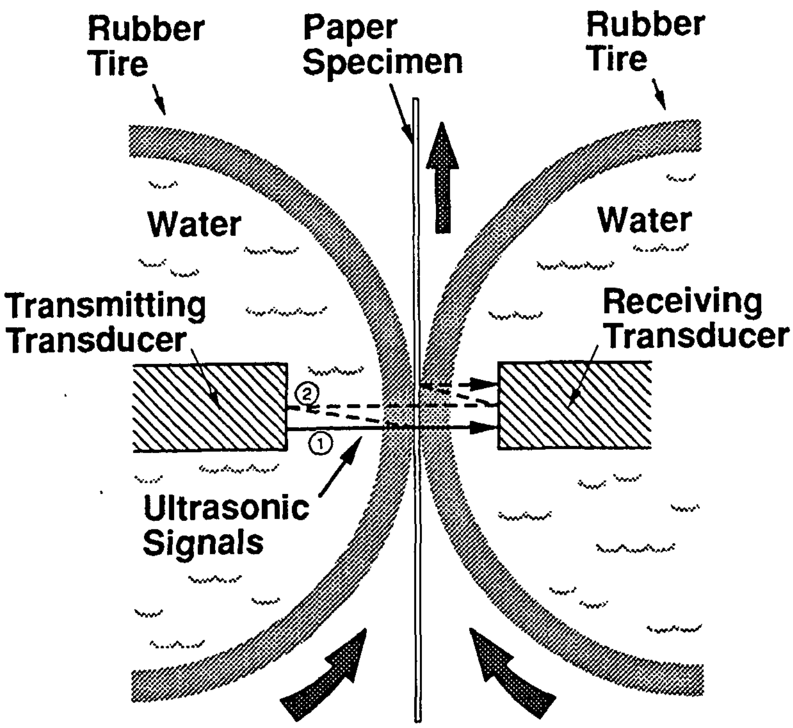

Figure 2: Schematic of the ultrasonic measurement technique.

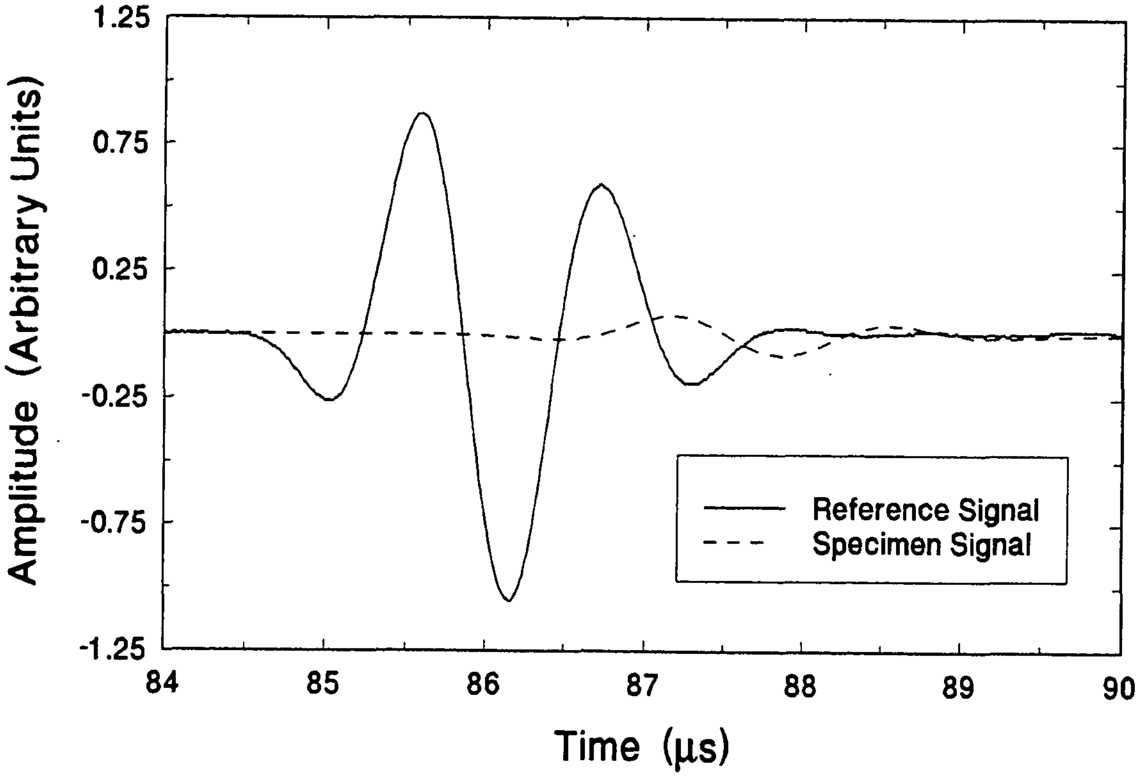

Figure 3: Time domain recordings of the directly transmitted signal collected without and with a specimen inserted in the nip between the wheels.

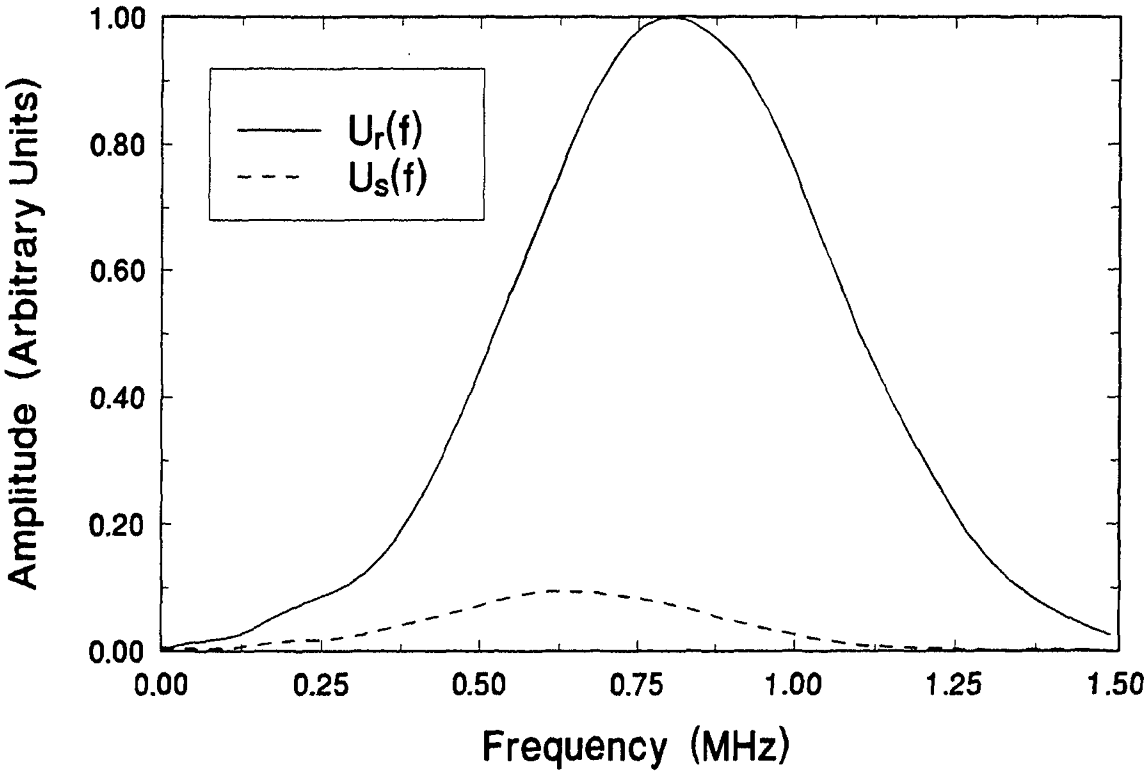

Figure 4: Frequency domain amplitude spectra for the reference and specimen waveforms.

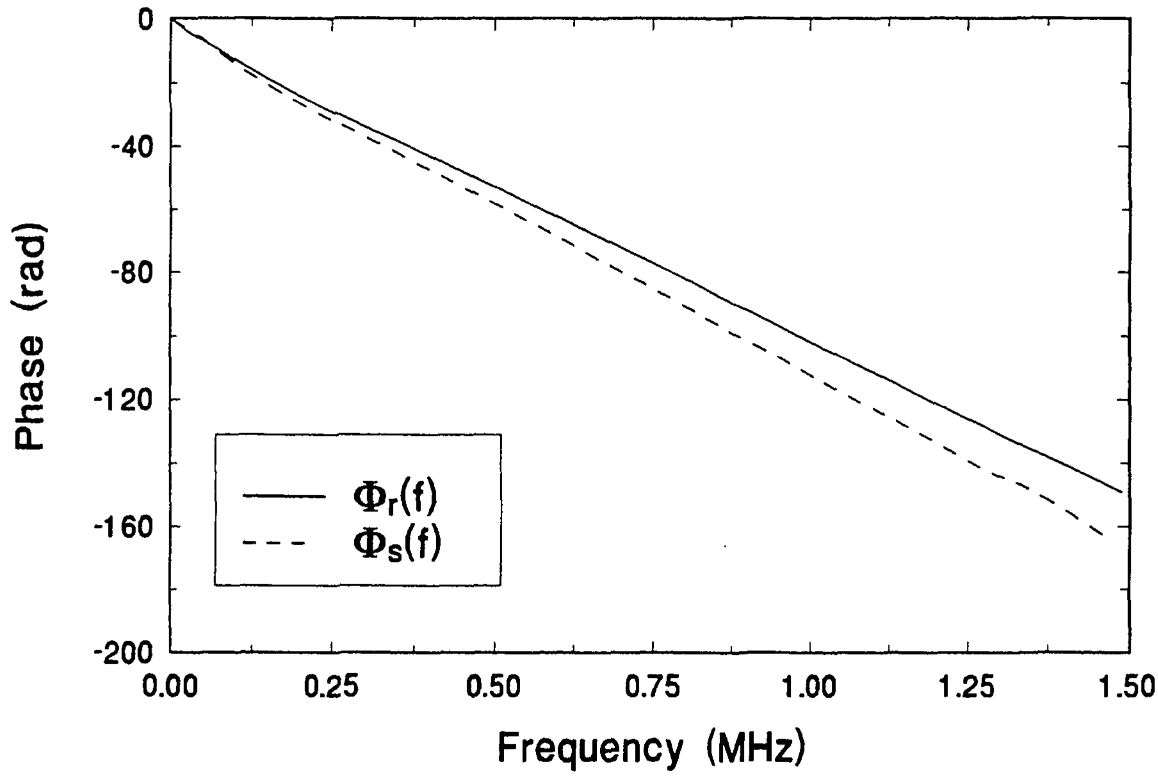

Figure 5: Phase spectra for the reference and specimen waveforms.

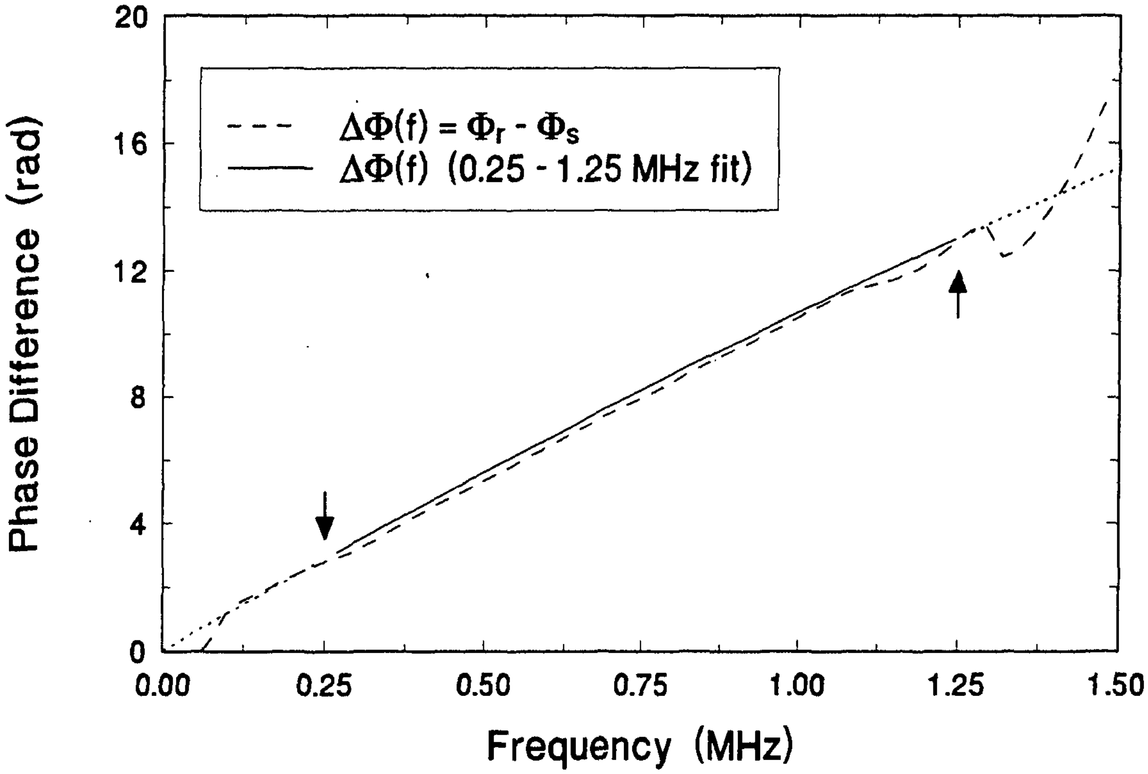

Figure 6: Difference between the reference and specimen phase spectra. The region delimited by the arrows corresponds to the selected region for curve fitting calculations.

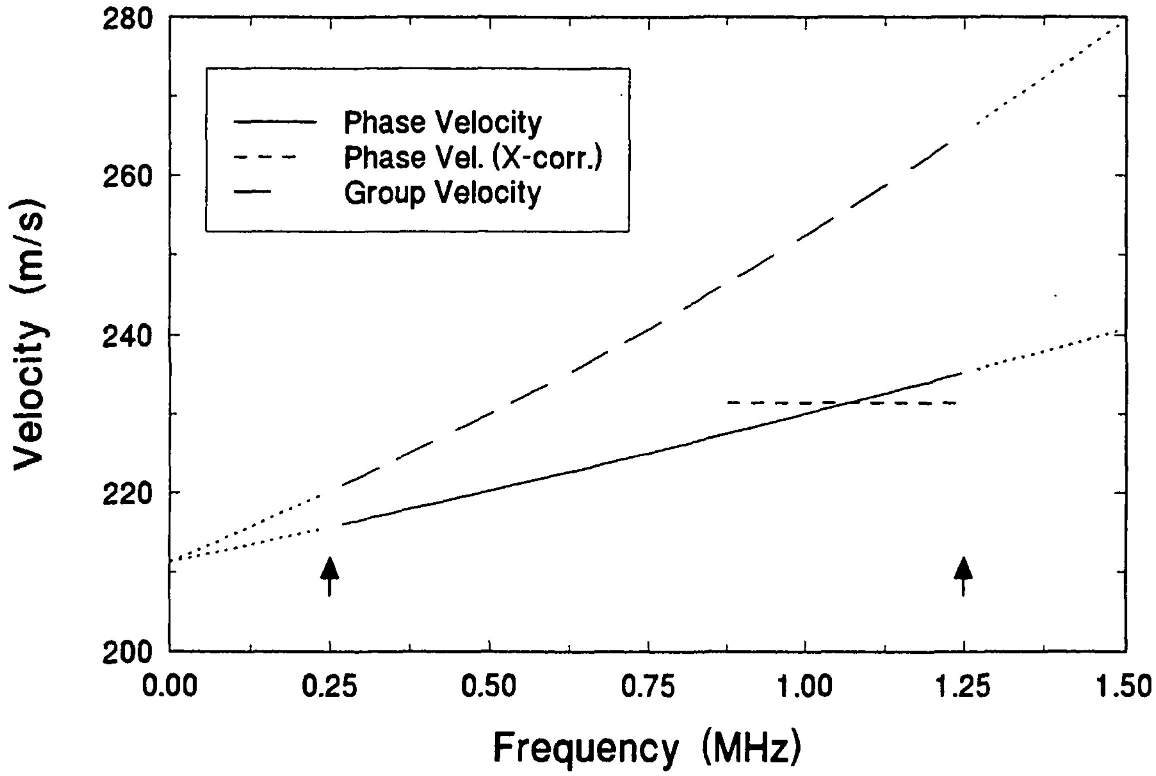

Figure 7: Sound dispersion information: phase and group velocities as a function of frequency. The short-dashed line represents the frequency independent out-of-plane velocity as obtained from cross-correlation calculations.

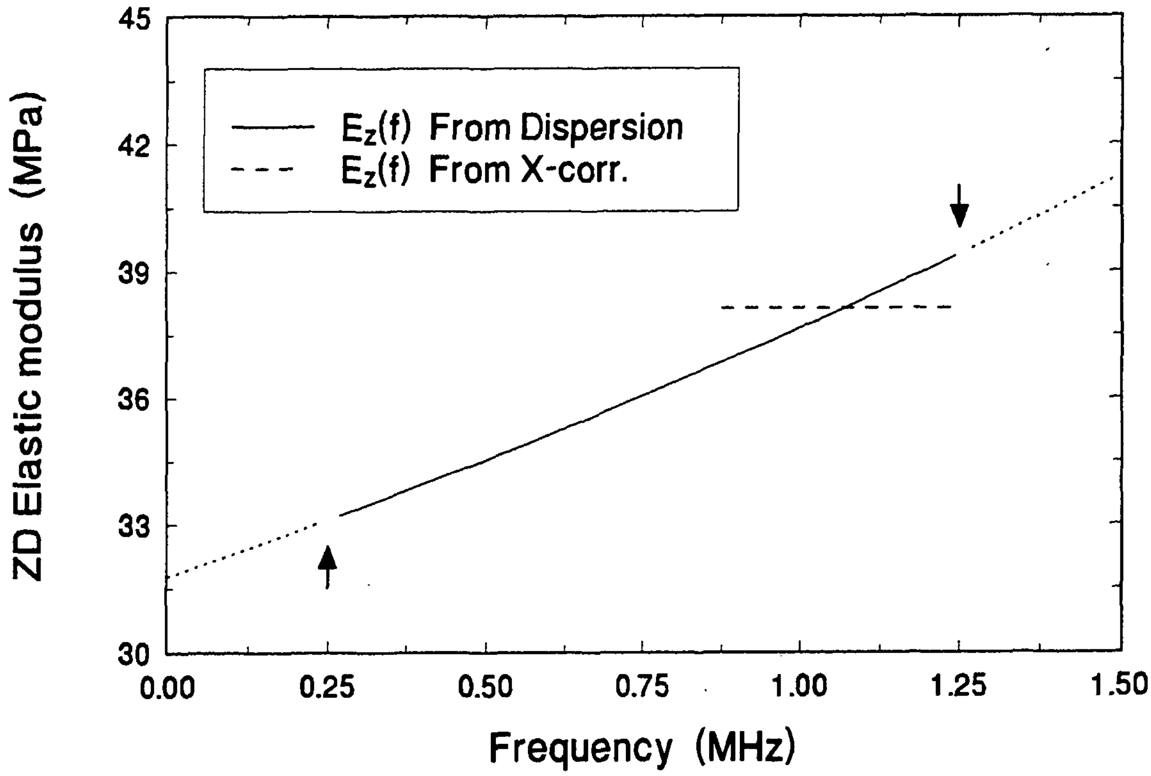

Figure 8: Z-direction elastic modulus as a function of frequency. The dashed line represents the frequency independent elastic modulus.

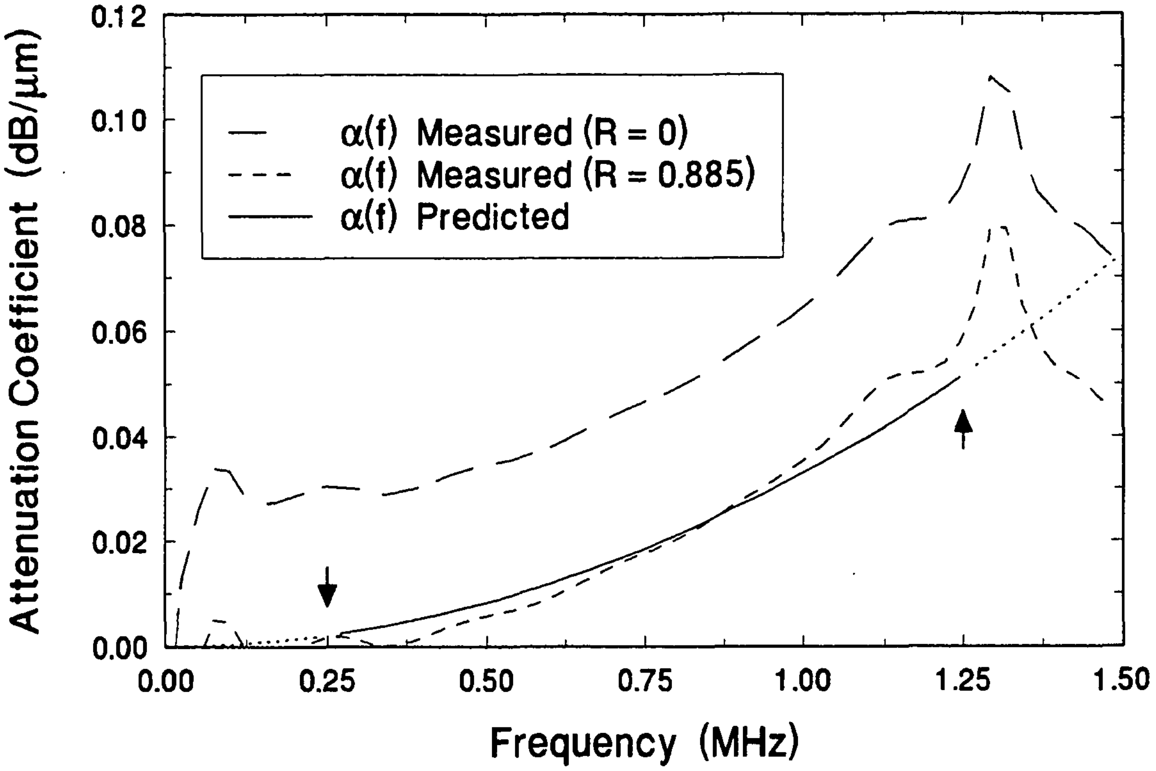

Figure 9: Sound attenuation information: measured and predicted attenuation coefficients as a function of frequency.

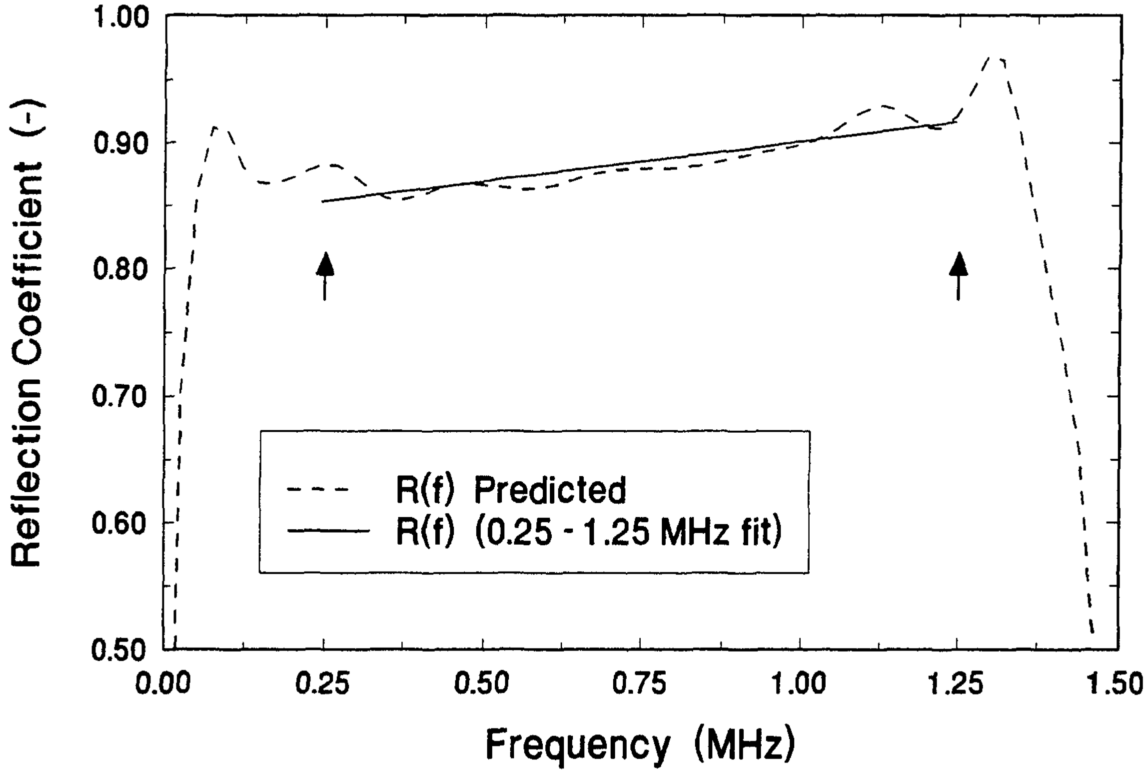

Figure 10: Sound reflection coefficient as determined from the comparative analysis of the measured and predicted attenuation coefficients.